Desalination and Water Treatment
www.deswater.com

doi: 10.5004/dwt.2018.23025

126 (2018) 67–72
September

Nanofiltration composite polymeric/ceramic membranes prepared from powder waste of ceramic tile kiln remnants

Shereen Kamel Amin[a], Heba Abdallah[a,*], Sahar S. Ali[a], Adnan Alhathal Alanezi[b,c]

[a]*Chemical Engineering Pilot Plant Department, Engineering Research Division, National Research Centre (NRC), 33 El-Bohouth St. (Former El-Tahrir St.), Dokki, Giza, Egypt, P.O. Box 12622, Affiliation ID: 60014618, Tel. 202 33335494; Fax: 202 33370931; emails: heba_nasr94@yahoo.com, drhebaabdallah3@gmail.com (H. Abdallah), dr.shereenkamel@hotmail.com, sheren51078@yahoo.com (Sh.K. Amin), sahar_saad_ali@yahoo.com (S.S. Ali)*
[b]*Department of Chemical Engineering Technology, College of Technological Studies, The Public Authority for Applied Education and Training (PAAET), P.O. Box 117, Sabah Al-Salem, 44010, Kuwait, email: aa.alanezi@paaet.edu.kw (A.A. Alanezi)*
[c]*Chemical and Process Engineering Department, Faculty of Engineering and Physical Sciences, University of Surrey, Guildford, UK*

Received 23 January 2018; Accepted 24 August 2018

ABSTRACT

Novel nano-filtration composite polymeric/ceramic membranes were successfully fabricated. The prepared membranes were prepared using powder from ceramic tile kiln remnants, which contain a high percentage of alumina. Support ceramic membranes samples were formed into discs by using polyvinyl alcohol organic binder. The top layer of the membrane was a polymeric solution of polyethersulfone. The prepared membrane exhibited good performance and the results indicated that the dye separation reached to 99.8% and 99.5% with a high permeate flux of 86 L/m^{2}h to 48.2 L/m^{2}h under an operating pressure of 8 bar, and the dye concentrations of 50 to 200 ppm, respectively, after 30 min.

Keywords: Ceramic membranes; Nanofiltration; Dye removal; Powder waste

1. Introduction

Microfiltration (MF) and ultrafiltration ceramic membranes have been successfully utilized for wide range of filtration processes such as separation of microorganisms, bacteria, colloidal solutes, and proteins. On the other hand, nanofiltration (NF) is applied most widely for water and wastewater treatment containing heavy metals and multiple synthetic dyes. Additionally, the application of ceramic membranes has recently been extended to non-aqueous solution separation, especially in petrochemical processing, where organic membranes cannot be utilized. It has also been interestingly applied in the separation and concentrations of organic solvents such as ethanol and hexane. Additionally, ceramic membranes can also be used in the separation of supercritical fluids, especially supercritical CO_2 and alcohol [1–3].

Low cost of the mineral-based porous ceramic membranes makes them under the circle of interest. Tubular ceramic membranes can be fabricated from an asymmetric configuration with coating on a porous support that offers good mechanical strength and thermal shock resistance, which is more desirable for difficult filtration applications such as gas separation [4–6]. The surface modification of ceramic membrane reduces the pore size of the membrane surface and can improve the hydrophilic behavior of membrane, such as fluoro-alkyl silanes that often used for modification [7–10]. Grafting process is the method which used to improve the surface nature of ceramic membranes to be hydrophilic or hydrophobic [7–11]. Hazardous wastes are produced from ceramic tile production and, to a lesser extent, flat dinnerware and pottery, where these products are fired in roller kilns. These kilns offer several advantages over conventional tunnel kilns: lower fuel consumption, computer-controlled

* Corresponding author.

firing curves, low maintenance due to lack of kiln cars, rapid firing cycles of less than 1 h, and the ability to shut down the kiln on very short notice [12–14]. One recurrent problem in the operation of such kilns is the necessity to grind the kiln rollers periodically. The high alumina grinding powder was contaminated by alkali salts depositions with condensation of the vapor phase. These latter salts, in turn, arise from the additions of the original ceramic body recipe to impart some specific properties [12–14]. In an average plant using one or two such kilns, the monthly product of grinding will consist of several tons of fine powder that usually accumulate within the plant premises as stockpiles. This represents an extremely high ecological hazard; for example, the powder if inhaled for long periods can lead to serious lung problems such as silicosis [14–20].

The novelty of this work is using the waste powder from the production of ceramic tiles which contains high percentage of alumina and is considered hopeless waste, in the production of ceramic support membranes.

The present article explains how the wastes from ceramic tiles are recycled and treated to be used in the preparation of supported ceramic membranes. A polymeric solution is used to produce the thin top membrane layer, which is considered the selective layer of the membrane. However, the parameters that affect the membrane production and characterization are studied to produce the best membrane structure that can be used in water treatment.

2. Experiment

2.1. Materials

Hazardous fine waste from kiln roller was supplied by Ceramica Prima Company, Sadat city, Egypt. Polyvinyl alcohol (PVA) was purchased from Sigma-Aldrich Company (USA). Polyethersulfone (PES; Ultrason E6020P with molecular weight 58,000 Da), supplied by BASF, Germany, was used as a polymer for preparation of the polymeric solution using the solvent N-methyl pyrrolidone (NMP), purchased from Sigma-Aldrich. Synthetic dye solutions were prepared using methylene blue, purchased from Merck (USA).

2.2. Characterization of the waste powder

2.2.1. Chemical analysis

X-ray fluorescence (XRF) analyses were run on an AXIOS Analytical 2005 wavelength dispersive (WD-XRF) sequential spectrometer, which is installed at the National Research Center, Egypt. The samples were crushed and then ground in a Herzog-type mill to realize a powder fine size. The samples were fabricated as pressed discs and then put in standard aluminum cups, using uniaxial pressing machine under total force of 130 kN.

2.2.2. Mineralogical analysis

For the X-ray diffraction (XRD) study, the sample was split into two aliquots, one for bulk mineral analysis and the other for clay analysis. The aliquot for bulk mineral analysis was finely ground (–200 mesh), mounted randomly on an aluminum holder, and analyzed by D8 ADVANCE X-ray diffractometer (Bruker, USA) apparatus with monochromatized Cu Kα radiation, operated at 40 kV and 40 mA. The diffractograms were used to provide background information on the bulk mineralogy of the sample, and particularly to estimate the relative abundance of the non-clay minerals in the sample.

2.2.3. Transmission electron microscopy

The powder samples were tested by transmission electron microscopy (TEM), where an image is made from the interaction of the electrons transmitted through the specimen using the JEM-2100 Plus instrument (JEOL, Japan).

2.2.4. Particle size distribution

The waste fineness and particle size distribution were investigated with laser particle size analyzer (BT-2001), which conforms to the International Standard ISO 13320 [21].

2.3. Preparation of composite ceramic membrane

Ceramic membrane preparation from the high-alumina grind waste was carried out as follows:

2.3.1. Preparation of PVA solutions

PVA powder (2 wt%) was directly added to the water at 90°C under mixing with a magnetic stirrer until the PVA was fully dissolved, then this solution was continuously mixed on cold for 1 h.

2.3.2. Preparation of support membrane specimens

Fine waste powder (10 g) was mixed with PVA solution 15 wt%. Cylindrical samples of diameter 50 mm were formed using lab automatic hydraulic press with uniaxial load of 5 ton (corresponding to a pressure of 25 MPa), then the samples were dried at temperature of 110°C ± 5°C overnight. Finally, they were fired at temperature of 1,100°C for a 1 h soaking time at a laboratory furnace with heating rates were chosen to be 10°C/min.

2.3.3. Top – layer preparation

PES polymeric solutions were prepared, where 12 wt% PES was dissolved in NMP, and the solutions were stirred for 3 h. Finally, the solution was sprayed on the ceramic membrane support, and then the prepared composite membranes were dried at 120°C for 30 min.

2.4. Characterization of composite ceramic membrane

2.4.1. Pore size distribution, total porosity, total pore area, and average pore diameter determination for membrane samples

Mercury porosimetry is a well-adapted method used to characterize the pore size distributions of MF ceramic membranes with the help of simple calculations. In this method, mercury is forced into the pores of dry sample. The quantity of mercury forced into the pores is determined with high accuracy at each pressure, which can be measured by means

of capacity variation induced by the reduction in the Hg column height connected to the measuring cell. The values of the pore radii r_p depend on the applied pressure as shown in the following equation derived from the modified Laplace equation (Washburn equation) [12,13]:

$$r_p = \frac{-2\gamma\cos\theta}{p} \quad (1)$$

r_p is the pore radius at each pressure, P is the applied pressure, θ is the contact angle of mercury and γ is the capacity variation. The specimens were introduced into the sample holder chamber of the equipment by micrometric pore size with the type number of 9320 version 2.08. The test was carried out using hydraulic pressure in the range of 0.0124 to 206.5 MPa which related to the pore radius values in the range of ~6 nm to ~100 μm.

2.4.2. Scanning electron microscopy

SEM images were done on the membrane surface, where ceramic membrane samples were coated with gold layer with thickness of 200–300 Å. SEM of samples was carried out using device (Quanta 250) FEG (field emission gun) under the potential difference of 30 KV.

2.5. Tests of dye separation

The filtration experiments were carried out using a lab filtration system technique, which had flat-sheet membrane module with three openings for feeding, recycling, and permeate. The methyl blue dye was continuously fed to the module from feeding tank by feeding pump of 0.8 MPa. The product was collected from the permeate side in collector tank. The experiments were performed using methylene blue dye with the concentrations of 50, 100, and 200 ppm. The dye solutions were prepared by dissolving the dye powder in distilled water. Samples were taken every 5 min for analysis. The operation of experiments was performed within 30 min at steady-state conditions. Analysis of the samples was carried out by UV analysis using a Shimadzu UV-visible spectrophotometer (HACH DR2800, Germany) to measure the light absorbency of the dye solution at a 660-nm wavelength.

The separation percentage of each species was calculated [11] as:

$$R = \left(1 - \frac{C_p}{C_R}\right) \times 100 \quad (2)$$

R is the separation (%), C_p is the solute concentration (dye concentration) in the permeate (mg/L), and C_R is the solute concentration (dye concentration) in the feed solution (mg/L); the permeate flux (J) of the membrane is calculated as follows:

$$J = \frac{Q}{(A \times t)} \quad (3)$$

J is the permeate flux (L/m^{2}h), Q is the permeate volume (L), A is the active surface area of the membrane (m^2), and t is time (h).

3. Results and discussion

3.1. Waste powder characterization

3.1.1. Chemical analysis

The chemical analysis of waste powder indicates that the high percentages of components were Al_2O_3 (63.86%), SiO_2 (23.55%), CaO (3.51%), ZrO_2 (3.45%), MgO (1.96%), Fe_2O_3 (1.16%), respectively [13,22]. Increasing in alumina percentage may be because of the rollers kiln materials made from high alumina grade. However, there is no observation of loss of ignition.

3.1.2. Mineralogical analysis

The waste powder mineralogical analysis is illustrated in Fig. 1. The result indicates that the waste composed of alumina (corundum) and mullite [13,22].

3.1.3. Transmission electron microscopy

TEM photos for the roller grind waste powder explain the formation of multilayers nanosheets of different lamellar crystal shapes as shown in Figs. 2(a) and (b). The lamellar crystal structure exhibits bright areas could be as an

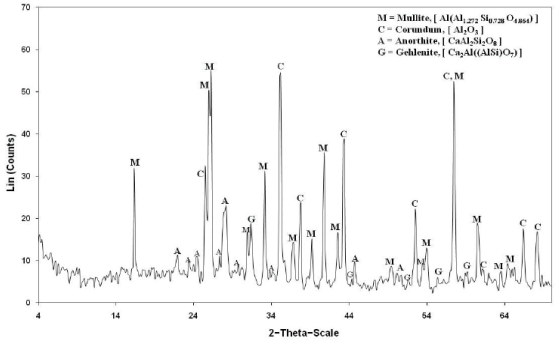

Fig. 1. XRD pattern of the waste powder [13,22].

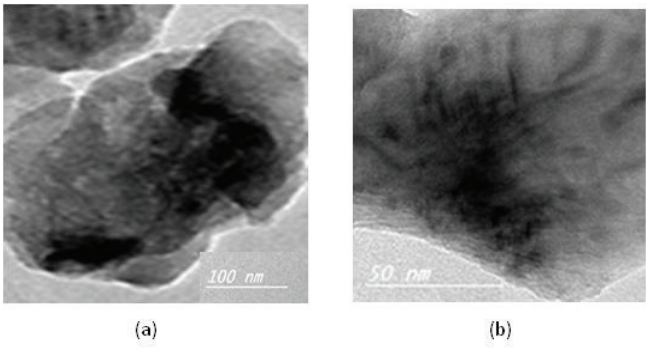

Fig. 2. TEM micrographs of waste powder; ((a) and (b)) lamellar crystal structure.

incomplete stacking with little mismatching in the layer superposition, this structure is determined by literature [22,23]. The dark areas in the image are related to the interface between various phases due to the difference in shapes and morphologies of raw powder waste. Also, the nucleation mechanism during the decomposition of the original ingredients includes expenditure of carbonates, quartz and clay minerals, which leads to recrystallization of aluminum–silicate, calcium–aluminum silicate (Gehlenite) and an aluminum oxide vitreous phase [23–31].

3.1.4. Particle size distribution of waste powder

The cumulative curve of waste powder particle size distribution explains that the waste powder has very soft granules as shown in Fig. 3, where the minimum particle size is about 300 nm, while the maximum value is about 200 μm and the medium particle size are approximately about 17 μm [13,22,23].

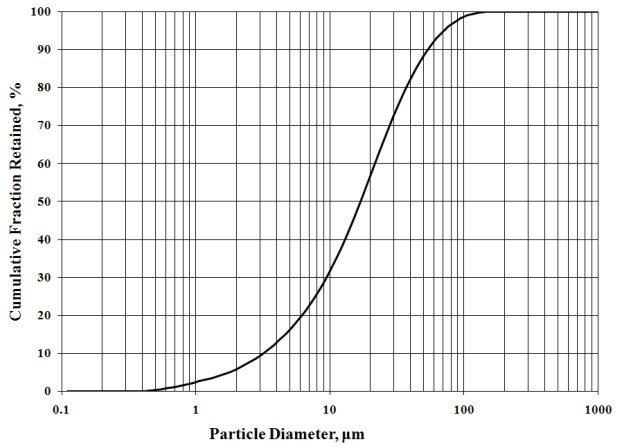

Fig. 3. Particle size distribution of waste powder [23,22].

3.2. Composite ceramic membrane characterization

3.2.1. Determination of the pore size distribution, average pore diameter, total porosity, and total pore area for ceramic membrane samples

The pore size distribution, average pore diameter, total porosity, and total pore area for ceramic membrane samples were determined by mercury porosimetry, where the results as follows, the mercury contact angle is 130°, total intrusion volume is 0.1882 mL/g, total pore area is 8.318 m^2/g, average pore diameter is 0.0905 μm, bulk density is 2.013 g/mL, porosity is 35.80%, and apparent specific gravity equal 3.14 g/mL. The pore size for the prepared membrane varied from 0.1 to 0.005 μm, so it can be used in nano-filtration applications.

On the other hand, Fig. 4 shows a photograph of the prepared membrane before and after drying. Fig. 4(a) indicates the wet polymeric layer on the membrane before drying. In Fig. 4(b), the color of the top membrane layer changed to white because of the coagulation of the polymeric layer on the top of the membrane.

3.2.2. Scanning electron microscopy

The SEM photos for prepared composite ceramic membrane are illustrated in Figs. 5(a) and (b), where the surface of the membrane has many nano-pores due to appreciable

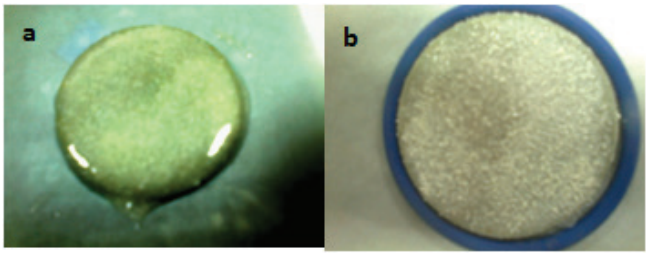

Fig. 4. Prepared composite ceramic membrane (a) before drying and (b) after drying.

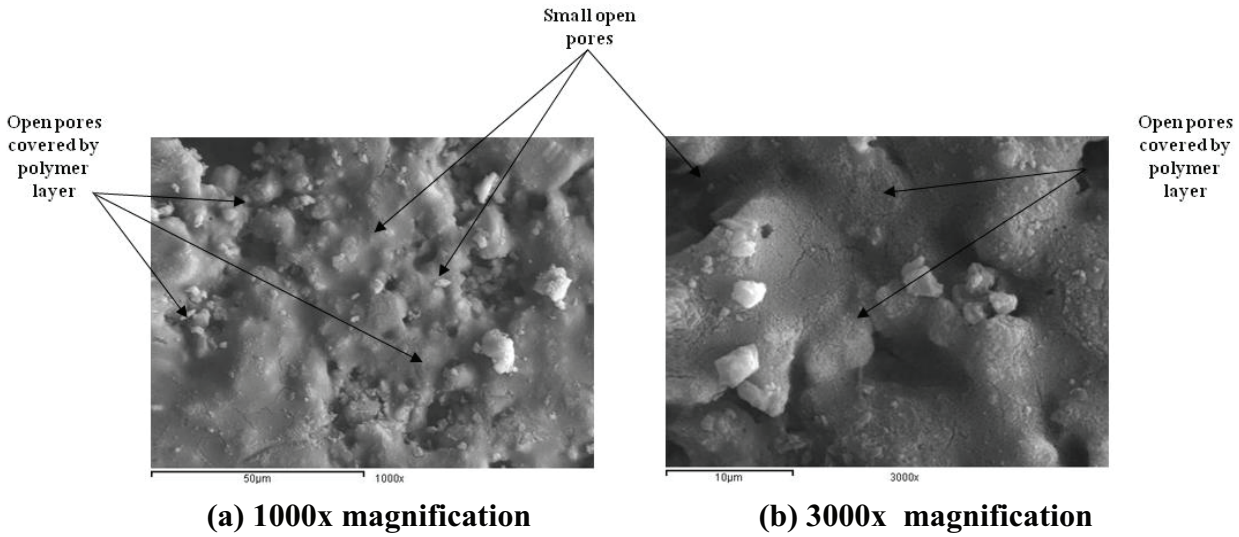

Fig. 5. SEM of prepared composite ceramic membrane. (a) 1,000x magnification and (b) 3,000x magnification

sintering setting temperature for firing ceramic membrane at 1,100°C. In addition, the surface of the membrane is coated with the layer of shiny glass; this is represented by the upper polymer layer. These results explain why the prepared composite ceramic membrane provided high performance.

3.3. Dye separation test

Fig. 6 illustrates the separation of dye during process time for methylene blue dyes at different concentrations of 50, 100, and 200 ppm at room temperature 25°C and operating pressure of 0.8 MPa. The figure shows that the separation of dye is positive according to the membrane active layer. Results indicate that the removal percentage reached to 99.8%, 99.5%, and 98.7% for dye concentrations of 50, 100 and 200 ppm, respectively, after 5 min from the beginning of the process, and slightly decreased with time due to clogging of the membrane pores with the increasing operation time. However, the permeate flux was increased at the beginning of the process time and decreased with increasing the process time until it reached to 86, 67.6, and 48.2 L/m^2 h for dye concentrations of 50, 100, and 200 ppm, respectively, after 30 min as shown in Fig. 7. The higher dye separation was obtained and slightly reduced with increasing operating time; that depends on the low solubility characteristics of the blue dye, which leads to membrane fouling at the end of the operation. The membrane fouling can be caused also, due to dye adsorption on the membrane surface observed during the experimental runs, which was observed by the presence of the blue color on the membrane after filtration.

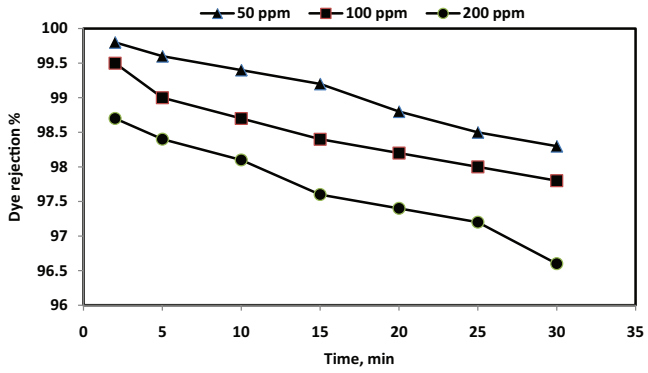

Fig. 6. Dye rejection using the prepared composite ceramic membrane.

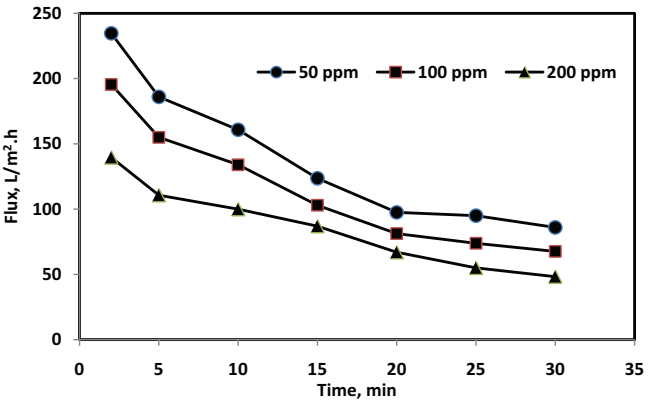

Fig. 7. Permeate flux of treated water using the prepared composite ceramic membrane.

Decreasing the flux with time is due to accumulation of dye on the surface of the membrane during operation forming a cake layer, this layer formed can perform an additional resistance to dye permeation but decrease the flux. Therefore, the permeate flux decreased and rejection increased as the operating time elapsed; this problem can be eliminated by washing or backwash of the membrane after flux decline [20].

4. Conclusion

Composite polymeric/ceramic membranes were successfully prepared using high-alumina waste powder from ceramic tile roller kilns. The prepared ceramic support was fired at temperature of 1,100°C using the soaking time of 1 h. The polymeric solution was sprayed on the top support surface.

The powder waste was analyzed by XRF for chemical composition, XRD for mineralogical composition, TEM, and particle size distribution. The results indicated that the powder contains high alumina percentage. The prepared composite polymeric/ceramic membrane was tested for dye separation. The results conducted that the dye removal percentage was 99.8%, 99.5%, and 98.7% for dye concentrations of 50, 100, and 200 ppm, respectively. Also, the permeate flux reached to 86, 67.6, and 48.2 L/m^2 h for dye concentrations of 50, 100, and 200 ppm, respectively, after 30 min. The permeate flux reduced with time due to the accumulation of dye on the membrane surface during operation forming a cake layer, which leads to decrease of the permeate flux, this problem can be eliminated by washing step or backwash step for membrane after flux decline.

Acknowledgment

The authors would like to acknowledge the Science and Technological Development Fund (STDF), Egypt, due to their financial support and all facilities they offered to perform this work, through the Project No. (10464), STDF – National Challenges Program.

References

[1] M. El-Kady, F. El-Shibini, Desalination in Egypt and the future application in supplementary irrigation, Desalination, 136 (2001) 63–72.
[2] R. Sharma, R. Agrawal, S. Chellam, Temperature effects on sieving characteristics of thin-film composite nanofiltration membranes: pore size distributions and transport parameters, J. Membr. Sci., 223 (2003) 69–87.
[3] M. Wiesner, S. Chellam, The promise of membrane technology, Environ. Sci. Technol., 33 (1999) 360A–366A.
[4] A. Verliefde, S. Heijman, E. Cornelissen, G. Amy, B. Bruggen, J. Van Dijk, Rejection of trace organic pollutants with high-pressure membranes (NF/RO), Environ. Prog., 27 (2008) 180–188.
[5] L. Nghiem, A. Manis, K. Soldenhoff, A.I. Schafer, Estrogenic hormone removal from wastewater using NF/RO membranes, J. Membr. Sci., 242 (2004) 37–45.
[6] C. Kim, H.G. Yoon, K.H. Lee, Formation of integrally skinned asymmetric polyetherimide nanofiltration membranes by phase inversion process, J. Appl. Polym. Sci., 84 (2002) 1300–1307.

[7] H.J. Kim, R.K. Tyagi, A.E. Fouda, K. Jonasson, The kinetic study for asymmetric membrane formation via phase-inversion process, J. Appl. Polym. Sci., 62 (1996) 621–629.
[8] Q.Z. Zheng, P. Wang, Y.N. Yang, D.J. Cui, The relationship between porosity and kinetics parameter of membrane formation in PSF ultrafiltration membrane, J. Membr. Sci., 286 (2006) 7–11.
[9] M. Amirilargani, E. Saljoughi, T. Mohammadi, M.R. Moghbeli, Effects of coagulation bath temperature and polyvinylpyrrolidone content on flat sheet asymmetric polyethersulfone membranes, Polym. Eng. Sci., 50 (2010) 885–893.
[10] A. Bhattacharya, B.N. Misra, Grafting: a versatile means to modify polymers: techniques, factors and applications, Prog. Polym. Sci., 29 (2004) 767–814.
[11] B. Wang, E.A. Jackson, J.W. Hoff, P.K. Dutta, Fabrication of zeolite/polymer composite membranes in a roller assembly, Microporous Mesoporous Mater., 223 (2016) 247–253.
[12] M.H. Roushdy, Sh.K. Amin, M.M. Ahmed, M.F. Abadir, Reuse of the product obtained on grinding kiln rollers in the manufacture of ceramic wall tiles, Ceram. Art Percept., 38 (2014) 60-66.
[13] Sh.K. Amin, M.H. Roushdy, S.A. El-Sherbiny, H.A.M. Abdallah, M.F. Abadir, Preparation of nano-size ceramic membrane from industrial waste, Int. J. Appl. Eng. Res., 11 (2016) 7176–7181.
[14] Sh.K. Amin, H.A.M. Abdallah, M.H. Roushdy, S.A. El-Sherbiny, An overview of production and development of ceramic membranes, Int. J. Appl. Eng. Res., 11 (2016) 7708–7721.
[15] L.S. Oliveira, A.S. Franca, M.T. Alves, S.D. Rocha, Evaluation of untreated coffee husks as potential bio-sorbents for treatment of dye-contaminated waters, J. Hazard. Mater., 155 (2008) 507–512.
[16] A. Chougui, K. Zaiter, A. Belouatek, B. Asli, Heavy metals and color retention by a synthesized inorganic membrane, Arab. J. Chem., 7 (2014) 817–822.
[17] A. Akbari, J.C. Remigy, P. Aptel, Treatment of textile dye effluent using a polyamide-based nanofiltration membrane, Chem. Eng. Process. Process Intensif., 41 (2002) 601–609.
[18] N. Saffaj, M. Persin, S. Alami-Younssi, A. Albizane, M. Bouhria, H. Loukili, H. Dach, A. Larbot, Removal of salts and dyes by low $ZnAl_2O_4$–TiO_2 ultrafiltration membrane deposited on support made from raw clay, Sep. Purif. Technol., 47 (2005) 36–42.
[19] N. Saffaj, S. Alami-Younssi, A. Albizane, A. Messouadi, M. Bouhria, M. Persin, M. Cretin, A. Larbot, Preparation and characterization of ultrafiltration membranes for toxic removal from wastewater, Desalination, 168 (2004) 259–263.
[20] I. Koyuncu, Reactive dye removal in dye/salt mixtures by nanofiltration membranes containing vinylsulphone dyes: effects of feed concentration and cross flow velocity, Desalination, 143 (2002) 243–253.
[21] ISO 13320/2009, Particle Size Analysis — Laser Diffraction Methods, International Organization for Standardization (ISO), Geneva, 2009, pp. 1–50.
[22] H. Abdallah, Sh.K. Amin, H.H. Abo–Almaged, M.F. Abadir, Fabrication of ceramic membranes from nano–rosette structure high alumina roller kiln waste powder for desalination application, Ceram. Int., 44 (2018) 8612–8622.
[23] H.H. Abo-Almaged, A.F. Moustafa, A.M. Ismail, Sh.K. Amin, M.F. Abadir, Hydrothermal treatment management of high alumina waste for synthesis of nanomaterials with new morphologies, Interceram Int. Ceram. Rev., 66 (2017) 172–179.
[24] M. Gemmi, M. Merlini, G. Cruciani, G. Artioli, Non–ideality and defectivity of the åkermanite–gehlenite solid solution: an X–ray diffraction and TEM study, Am. Mineral., 92 (2007) 1685–1694.
[25] M.J. Trindade, M.I. Dias, J. Coroado, F. Rocha, Mineralogical transformations of calcareous rich clays with firing: a comparative study between calcite and dolomite rich clays from Algarve, Portugal, Appl. Clay Sci., 42 (2009) 345–355.
[26] J.M.M. Molenaar, L. Katgerman, W.H. Kool, R.J. Smeulders, On the formation of the stircast structure, J. Mater. Sci., 21 (1986) 389–394.
[27] T.P. Schulze, S.H. Davis, Shear stabilization of morphological instability during directional solidification, J. Cryst. Growth, 149 (1995) 253–265.
[28] A. Aras, The change of phase composition in kaolinite and illite–rich clay–based ceramic bodies, Appl. Clay Sci., 24 (2004) 257–269.
[29] S.J. Louisnathan, Refinement of the crystal structure of a natural Gehlenite $Ca_2Al(AlSi)_2O_7$, Can. Mineral., 10 (1971) 822–837.
[30] C.L. Lo, J.G. Duh, B.S. Chiou, W.H. Lee, Microstructure characterization for Anorthite composite glass with nucleating agent of TiO_2 under non–isothermal crystallization, Mater. Res. Bull., 37 (2002) 1949–1960.
[31] M.P. Riccardi, B. Messiga, P. Duminuco, An approach to the dynamics of clay firing, Appl. Clay Sci., 15 (1999) 393–409.